

# Error Backpropagation Neural Network Based Image Identification for a Foot Massage Machine and Its Mechanism Design

Chun-Chieh Wang

National Yunlin University of Science and Technology, 123 University Road, Section 3, Douliou, Yunlin 64002, Taiwan

E-mail: bigjasonwang@gmail.com

<https://www.yuntech.edu.tw/>

## Abstract

In the past twenty years, many companies have developed different styles of foot massage machines. At present, the common massage products on the market include roller type and pressing type. However, it is very difficult to accurately stimulate all acupuncture points for different sizes of feet. Besides, the massage roller cannot be controlled independently. Therefore, a novel computer vision technology is proposed to identify the foot acupuncture points by error backpropagation neural network (EBNN) in this paper. First, we use cameras to capture the sole of users' soles and execute image preprocessing procedures to segment the region of interest (ROI) of soles. We map foot acupuncture points to foot images to obtain reference massage positions. Second, the YCbCr color space is used to separate the brightness to complete the segmentation of the foot image in the skin detection. Moreover, EBNN is used to train users' soles-image sets to improve the success rate of image segmentation. Finally, to improve the rate of image recognition and user convenience, a foot massage machine was redesigned. Experimental results validate the superiority and practicality of the proposed image identification method for foot massage machines.

**Keywords:** Error backpropagation neural network (EBNN), Foot massage machines, Image identification

## 1. Introduction

Dr. Fitzgerald proposed the concept of foot reflexology massage in 1913 [1]. It wasn't until the 1970s that foot massage techniques received the attention of the medical community. Since ancient times, the concept of acupuncture points corresponding to body organs is used in the traditional Chinese medicine therapy. Therefore, to combine the concept of reflexology and acupuncture points, many companies have developed different styles of foot massage machines in the past two decades. The current products on the market contain two kinds of forms of massage, roller-type and push-type.

The rotate-type massage machines can fit different feet, but the rollers are limited in certain massage areas. Moreover, for the push-type massage machines, it is difficult to accurately stimulate all acupuncture points for different foot shapes. Besides, the massage roller cannot be controlled independently. Therefore, for the research of foot massage machines, how to find the corresponding acupuncture points will be the most problem to be overcome.

The foot reflexology map that is most often referred to in the development process of the foot massage machine

[2], as shown in Fig. 1. The author hopes to design a foot massage machine that can give corresponding force to different acupuncture points. However, the existing foot massage machines are usually designed for the foot shape of adults. Not only that, but most of the machines cannot accurately press all the acupuncture points.

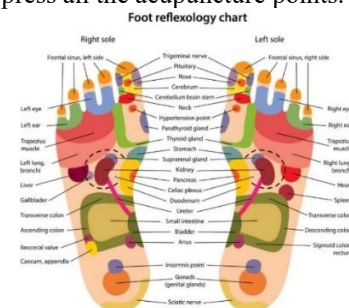


Fig. 1. Foot reflexology chart [2]

To overcome the above problems, the author used EBNN to detect foot acupuncture points. The key steps consist of three parts. First, a camera is used to capture the sole of the users' soles. An image preprocessing procedure is performed to segment ROI of the sole. To get the position of the reference massage, the foot

acupuncture points are mapped onto the foot image. Second, to complete the segmentation of the foot image, the YCbCr color space is used in skin detection to separate the brightness. Furthermore, the shoe sole image set is trained using EBNN to improve the success rate of image segmentation. Finally, to realize all acupuncture points massage function, an FPGA/DSP embedded system will be used for image processing and multi-axis PWM control. The results verify the superiority and practicality of the proposed image detection method for foot massage machines.

## 2. Hardware architecture design

### 2.1. Mechanism design

To improve the rate of image recognition and user convenience, a foot massage machine is re-designed, shown as Fig. 2. In our design, the foot massage machine is portable. Fig. 2(a)-(b) shows the drawbars pull up and drop down, respectively.

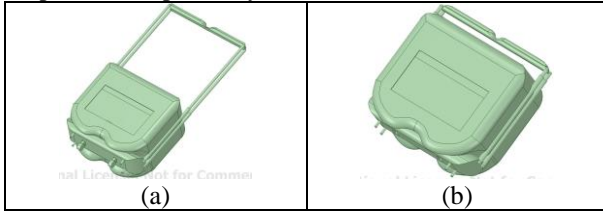


Fig. 2. Foot massage machine body 3D design

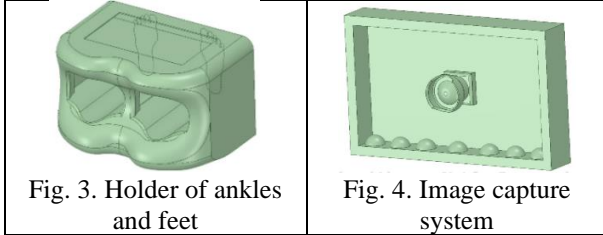


Fig. 3. Holder of ankles and feet

Fig. 4. Image capture system

The overall design includes four parts: a holder of ankles and feet (shown as Fig. 3), an image capture system (shown as Fig. 4), a massage institution (shown as Fig. 5), and embedded electronic control devices.

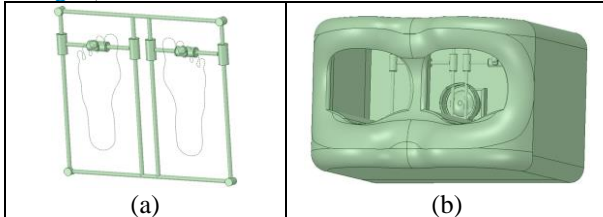


Fig. 5. Massage institution

The holder is designed to meet the general adult feet. Fig. 5(a) shows the massage buttons and x-y axis connecting bars. The x-y axis connecting bars drive by servo motors. The massage buttons can reach all foot acupuncture points by x-y axis connecting bars. The foot massage machine assembly is shown as Fig. 5(b). Moreover, to facilitate the implementation of image

recognition system, some special airbags are used to fix the different size feet. After above procedures, we use a DSP-FPGA hybrid embedded system to get the coordinates of the plantar acupuncture points. At the same time, the embedded system drives a proposed mechanism in order to make precise compressions on these acupuncture points. In addition, an LCD module (shown as Fig. 6) will show the location of acupuncture points, treatment time, and the related physical information.



Fig. 6. LCD module

### 2.2. DSP-FPGA hybrid embedded system

In this paper, the DSP-FPGA hybrid embedded system is proposed. FPGA is used for video encoding and image preprocessing calculations. DSP is used for acupuncture points mapping and massage mechanism controlling. The architecture is shown in Fig. 7.

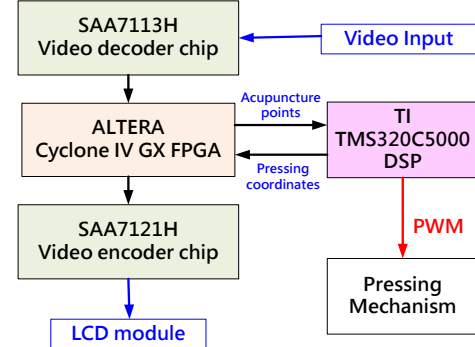


Fig 7. DSP-FPGA Hybrid Embedded System

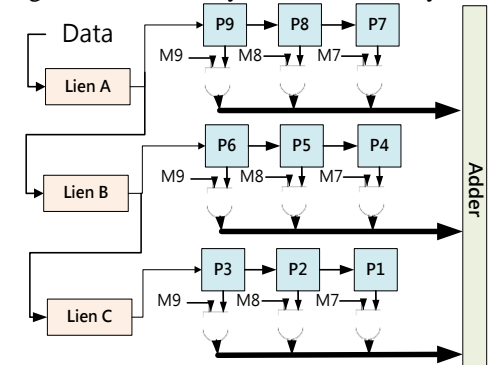


Fig. 8.  $3 \times 3$  Mask Convolution Operation

A 3 by 3 masked convolution operation is used for edge detection. Data extraction [3] is shown in Fig. 8. In

this paper, line buffer is used to fetch row data to reduce the register requirement. Furthermore, the length of line buffer can be regulated for different image size.

### 3. Acupuncture points detection via computer vision

#### 3.1. Foot reflexology image segmentation

Color model and brightness compensation are the two main processes of the foot reflexology image segmentation. The  $YC_bC_r$  color model is used to achieve plantar reflexology image segmentation [4]. ( $Y$  is the brightness,  $C_b$  and  $C_r$  are blue and red intensities, respectively.) Besides, given that light compensation is still not done for most images. For this reason, Zhang [5] proposed an adaptive brightness compensation method. The formula is as follows.

$$L_c = \frac{H_{std}}{D_{avg}} \quad (1)$$

where

$$H_{std} = \frac{\sum_{i=1}^i [\max(V_R, V_G, V_B) + \min(V_R, V_G, V_B)]}{2 \times j} \quad (2)$$

$$j = i - \sum_{i=1}^i (V_R = V_G = V_B = 0)$$

$H_{std}$  can be changed with different images.  $i$  is the amount of pixels in an image.  $j$  is the number of non-black pixels in the image.  $V_R$ ,  $V_G$  and  $V_B$  are the red, green, and blue components of the pixel, respectively.  $D_{avg}$  is the non-black pixels of  $V_R$ ,  $V_G$  and  $V_B$ . In addition, to obtain training data, EBNN [6][7][8][9] is used. The EBNN segmentation process is shown in Fig. 9.

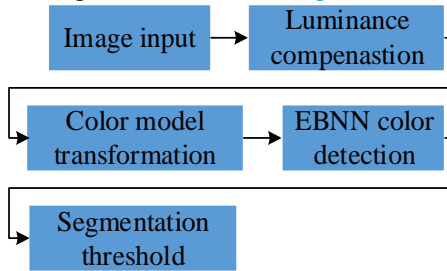


Fig. 9. EBNN Segmentation Process.

The algorithm of EBNN is described in the following steps.

Step 1. Set all the weights and threshold levels of the neural network so that the random numbers can be evenly distributed over a small range.

#### 【Feedforward】

Step 2. Deliver the training data ( $YC_bCr$ ) to the input node of the training cycle.

Step 3. Calculate the value of hidden nodes.

Step 4. Calculate the value of output nodes.

#### 【Backpropagation of the network error】

Step 5. Compares the actual value of each output node with the desired output value and calculates the squared error for each output node. (For each output node, send the squared error back to the hidden node.)

Step 6. Adjusts the weights linked to each output node based on the calculated squared error for each output node.

Step 7. The weights on the links to each hidden node are adjusted according to the squared error from the output node.

Step 8. When "stop condition" is false, return to step 2.

#### 3.2. Foot image obtaining and edge detection

To reduce computation time, the ROI of the plantar image is segmented. Furthermore, to find out the mapping range of acupuncture points, the edges of the foot image need to be calculated. Because the foot images are all curves, the detection results will produce many discrete segments. Therefore, LoG (Laplacian of Gaussian) operator is used for curves edge detection in this paper.

Second-order Laplace function is

$$\nabla^2 L = \frac{\partial^2 L}{\partial x^2} + \frac{\partial^2 L}{\partial y^2} \quad (3)$$

and Gaussian function is

$$G(r) = -e^{-\frac{d^2}{2\sigma^2}} \quad (4)$$

where  $d^2 = x^2 + y^2$ ,  $\sigma$  is the standard deviation. Laplacian of Gaussian operator is as follows.

$$\nabla^2 LoG(r) = -\left[ \frac{d^2 - \sigma^2}{\sigma^4} \right] e^{-\frac{d^2}{2\sigma^2}} \quad (5)$$

#### 3.3. Acupuncture points detection

The projective transformation of a two-dimensional plane [10] can be represented by a homogeneous vector as shown below.

$$\begin{bmatrix} a'_1 \\ a'_2 \\ a'_3 \end{bmatrix} = \begin{bmatrix} v_{11} & v_{12} & v_{13} \\ v_{21} & v_{22} & v_{23} \\ v_{31} & v_{32} & v_{33} \end{bmatrix} \begin{bmatrix} a_1 \\ a_2 \\ a_3 \end{bmatrix} \quad (6)$$

Assume that the corresponding non-homogeneous coordinates of two points on the plane are  $(a, b)$  and  $(a', b')$ . Then  $(a', b')$  can be calculated by Eq. (6), as shown in Eq. (7).

$$\begin{aligned}
 a' &= \frac{a'_1}{a'_3} = \frac{v_{11}a + v_{12}b + v_{13}}{v_{31}a + v_{32}b + v_{33}} \\
 b' &= \frac{a'_2}{a'_3} = \frac{v_{21}a + v_{22}b + v_{23}}{v_{31}a + v_{32}b + v_{33}}
 \end{aligned} \quad (7)$$

Solving equation (7) requires at least six corresponding points. Thus, standard foot acupuncture points can be mapped to the user's foot.

#### 4. Experimental results

In the paper, the foot image is cut into three mapping ranges. Range 1: Range 2: Range 3=3.5:3:3.5 (Fig. 10). Range 1, Range 2 and Range 3 cover 12, 7 and 4 main acupuncture points respectively.

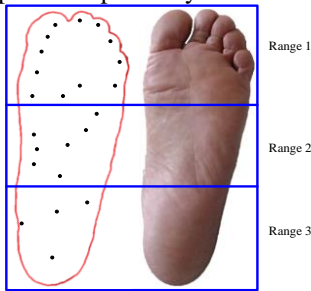


Fig. 10. Definition of Mapping Ranges

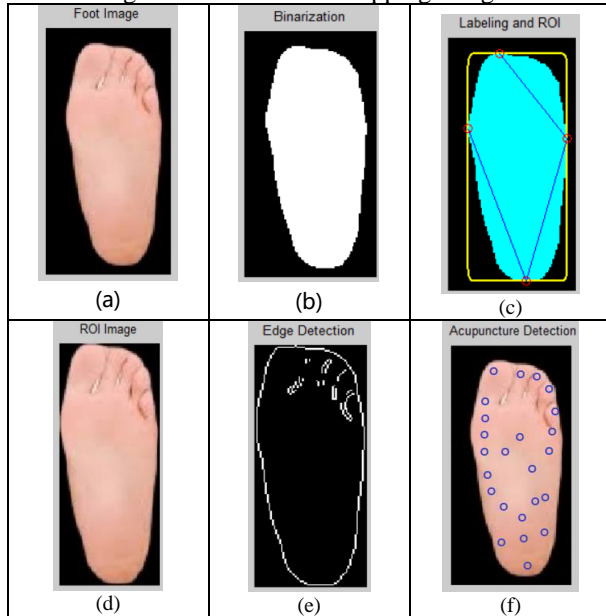


Fig. 11. Results of Image Processing and Acupuncture Points Mapping

Fig. 11 shows the results of image processing and acupuncture points mapping. Fig. 11(b) shows the skin color segmentation results of EBNN. The results verify that the foot image segmentation is clear.

#### 5. Conclusion

In this paper, a novel computer vision technique is proposed to identify foot reflexology points via EBNN. A camera is used to capture the sole of the users' foot. Moreover, an image preprocessing procedure is performed to segment ROI of the soles. Foot reflexology points are mapped to foot images to obtain reference massage positions. In addition, the YCbCr color space is used to separate the brightness to complete the segmentation of the foot image in the skin detection. Moreover, EBNN is used to train the user's shoe sole image set to improve the success rate of image segmentation. Not only that, but a foot massage machine has been redesigned to improve the image recognition rate and user convenience. The experimental results verify the superiority and practicability of the proposed image recognition method for foot massage machines.

#### References

- [1] Kaye A., Mathan DC (1980), *Reflexology for Good Health*, Wilshire Book Co.
- [2] <https://cloudmassage.com/blogs/news/the-main-pressure-points-on-our-feet-and-what-they-mean-a-basic-guide>
- [3] P.Y. Hsiao, C.H. Chen, H. Wen and S.J. Chen (2006), Real-time realisation of noise-immune gradient-based edge detector, *IEE Proceedings on Computers and Digital Techniques*, 153(4): 261-269.
- [4] Zhang S, Jing X, Zhang B, Sun S (2010), An Adaptive Fingerprint Image Segmentation Algorithm Based on Multiple Features, *Advanced Computer Control*, pp.191-194.
- [5] Zhang D, Zhoua ZH, Chen S (2005), Diagonal principal component analysis for face recognition, *Pattern Recognition Society*, 39(1):140-142.
- [6] Rojas R. (1996), *Neural Networks - A Systematic Introduction*, Springer.
- [7] Anthony M., Bartlett P. L. (2009), *Neural Network Learning: Theoretical Foundations*, Cambridge University Press
- [8] Andrés B.C., Pedro J. G.L., José-Luis S.G. (2013), Neural architecture design based on extreme learning machine, *Neural Networks*, 48:19-24.
- [9] L.G. Wright, T. Onodera, M.M. Stein, T. Wang, D.T. Schachter, Z. Hu, P.L. McMahon (2022), Deep physical neural networks trained with backpropagation, *Nature*, Vol. 601, 549-555.
- [10] Hartley R, Zisserman A(2004), *Multiple View Geometry in Computer Vision*, 2nd Edition, Cambridge University Press.

---

---

### **Authors Introduction**

Prof. Chun-Chieh Wang



He is a professor of National Yunlin University of Science and Technology. His areas of research interest include robotics, image detection, electromechanical integration, innovative inventions, long-term care aids, and application of control theory. He is now a permanent member of Chinese Automatic Control Society (CACS) and Taiwan Society of Robotics (TSR). He is also a member of Robot Artificial Life Society.